Physical Biology

PAPER

Static mechanical strain induces capillary endothelial cell cycle re-entry and sprouting

A S Zeiger[1,2], F D Liu[2,3], J T Durham[4], A Jagielska[1], R Mahmoodian[1], K J Van Vliet[1,2,3,5] and I M Herman[4,5]

1   Department of Materials Science & Engineering, Massachusetts Institute of Technology, Cambridge, MA 02139
2   BioSystems & Micromechanics Interdisciplinary Research Group (BioSyM), Singapore-MIT Alliance in Research & Technology (SMART), Singapore 138602
3   Department of Biological Engineering, Massachusetts Institute of Technology, 77 Massachusetts Avenue, Cambridge, MA 02139 USA
4   Graduate Program in Cell, Molecular and Developmental Biology, Sackler School of Graduate Biomedical Sciences and Center for Innovations in Wound Healing Research, School of Medicine, Tufts University, 150 Harrison Avenue, Boston, MA 02111 USA
5   Authors to whom any correspondence should be addressed.

Abstract

Vascular endothelial cells are known to respond to a range of biochemical and time-varying mechanical cues that can promote blood vessel sprouting termed angiogenesis. It is less understood how these cells respond to sustained (i.e., static) mechanical cues such as the deformation generated by other contractile vascular cells, cues which can change with age and disease state. Here we demonstrate that static tensile strain of 10%, consistent with that exerted by contractile microvascular pericytes, can directly and rapidly induce cell cycle re-entry in growth-arrested microvascular endothelial cell monolayers. S-phase entry in response to this strain correlates with absence of nuclear p27, a cyclin-dependent kinase inhibitor. Furthermore, this modest strain promotes sprouting of endothelial cells, suggesting a novel mechanical 'angiogenic switch'. These findings suggest that static tensile strain can directly stimulate pathological angiogenesis, implying that pericyte absence or death is not necessarily required of endothelial cell re-activation.

Introduction

Microvascular endothelial cells (EC) are understood to respond to various extracellular mechanical cues. However, the role of sustained (static) mechanical tension to EC monolayers, as could be generated by adjacent cell types in the microvasculature, is less understood. For example, dynamic mechanical cues such as fluid shear stress [1–3] and cyclic strain from transmural or pulse pressure [4–7] have long been considered dynamic contributors to vascular cell (dys)function in larger vessels such as arteries and veins. Static tensile force and strain [8–11] have also been shown to alter proliferation or migration of non-confluent EC cultures *in vitro*; however, such ECs are not in the growth-arrested state typical of the non-sprouting microvasculature. Other studies that include vessel fragments [8], multiple cell types, or *in vivo* implantation [12, 13] suggest that either mechanical constraints to or cell-generated deformation of the extracellular matrix can modulate at least neovessel network formation; however, these approaches also obfuscate decoupling of mechanical cues from biochemical cues associated with inflammation, wound healing, and paracrine signaling. Thus, it has remained unclear whether and how well-controlled, simple strain states could induce a phenotypic transition in ECs to promote angiogenesis, the sprouting of new vessels from existing vasculature. In particular, it remains unknown how the static strains that have been reported to be generated by contractile microvascular pericytes may contribute to EC growth dynamics, including angiogenic sprouting from intact EC monolayers [14, 15].

Pericytes are the predominant contractile cell type in microvessels, encircling venular and capillary ECs and communicating in close physical contact while embedded within the basement membrane [14, 16]. Interactions between pericytes and associated EC are considered critical to microvasculature growth,

stabilization, and survival, though most prior work has focused on biochemical aspects of this interaction [15, 17]. Specifically, pericytes can inhibit vascular EC proliferation, foster microvascular stabilization and influence barrier function through cell contact- and paracrine mediator-dependent mechanisms [14, 18]. These cells express cytoskeletal and contractile proteins [19]; and mechanical contraction by these cells has been quantified [17] and linked to the RhoGTPase effector pathway [18, 20]. We have shown previously that pericytes can exert a sustained contractile force that results in the mechanical deformation of extracellular materials [14, 17, 18]; this mechanical cue can stiffen the basement membrane [17] and can presumably be transferred to adjacent ECs. Such contractile force *in vivo* may result in an effective tensile strain on adjacent ECs located distal to the pericytes surrounding the microvessel walls [17].

Interest in this potential for mechanical modulation of EC monolayers is twofold. First, understanding how and when a cue such as static extracellular tension is transduced to a cell response within EC monolayers informs our framework for physical biology of strain-induced cell cycle re-entry and angiogenesis. Second, such findings can inform the debate of pericytes' role in vascular pathologies. Previous research has shown that the loss of pericytes, or 'pericyte dropout', is correlative with proliferative diabetic retinopathy [21–24]. However, other work suggests pericyte dysfunction—rather than death or loss—represents an early, initiating event in microvascular destabilization and pathological angiogenic activation [14, 25]. Moreover, we have shown via *in vitro* co-culture that molecular manipulation, which increased pericyte contractility correlated with loss of EC quiescence [20, 26], and can also promote angiogenic activation and microvascular sprouting [26]. To our knowledge, approaches have not been established to test the capacity for this isolated cue—sustained mechanical strain such as that generated by pericytes—to modulate capillary EC monolayer growth dynamics or angiogenic switching. Here, we demonstrate that static uniaxial strain, of magnitudes shown previously to be exerted by microvascular pericytes [18], is sufficient to induce S-phase re-entry in confluent and growth-arrested capillary-derived EC monolayers. This significant shift from growth-arrest toward proliferation occurs within 15 min post-strain, and correlates with diminution of nuclear p27, a cyclin-dependent kinase inhibitor and cell cycle regulator. We further show that this static mechanical strain is sufficient to induce angiogenic sprouting *in vitro*. These results indicate that mechanical deformation such as that initiated by pericyte contraction can signal EC cell cycle re-entry and potentially pathological angiogenic re-activation.

Experimental methods

Preparation of tissue culture polydimethylsiloxane (PDMS) molds

Details of design and testing of PDMS molds are described in the supporting information. To construct PDMS multi-well molds, lids of 48-well tissue culture polystyrene plates (#677180, Greiner Bio-One) were lined with parafilm (Bemis, Neenah, WI); the lid served simply as a template on which to construct molds of precise position and spacing. Sixteen 1.25 cm-diameter mosaic mirrors (SKU8224, KitKraft, Studio City, CA) were adhered to parafilm using ethyl cyanoacrylate-based epoxy (Pacer Technology, Rancho Cucamonga, CA) to match the inscribed patterns in the four rows and columns in the center of multi-well tissue culture polystyrene lids (#677180, Greiner Bio-One). These mirrors served as a negative template or mold for a sixteen well-plate. After allowing the adhesive to cure for 15 min at room temperature, mirrors were gently wiped clean with Kimwipes (Kimberly-Clark, Roswell, GA) soaked in ethanol. Chemically curable PDMS (Sylgard 184, Dow Corning Corporation) was prepared at a weight ratio of 20:1 base to curing agent and stirred vigorously for 3 min Mixed silicone of 25 ml volume was added to each of the prepared sixteen well molds and allowed to spread under 0.08–0.09 MPa of vacuum pressure in a vacuum oven for 30–60 min to degas and remove air bubbles. After removing all air bubbles, vacuum was released and the PDMS was then cured at 45 °C for 24–48 h. After baking, molds were soaked in acetone at room temperature for 24 h to remove any uncrosslinked PDMS, a modified version of the methods outlined by Vicker's *et al* [27]. Molds were then placed in an oven for ~24 h to evaporate and dry the acetone from the PDMS molds. PDMS molds were then sterilized with ethanol and allowed to dry under UV light. After sterilization and drying, the surface of the PDMS mold was then plasma oxidized (handheld corona device #12051A-10, Electro-Technic Products, Inc., Chicago, IL) for 60 s per mold, ensuring as uniform exposure to each well as possible. Such treatment allowed for the creation of hydrophilic PDMS for tissue culture (TC-PDMS) that retained hydrophilicity for at least 1 day in air and 14 days in fluids such as PBS or cell culture media. Note that cells can be seeded directly in these molded wells without the requirement of additional extracellular matrix proteins or surface functionalization chemistries [28]; this minimizes the potential for biased influence of exogenous adsorbed ECM proteins on cellular morphology or Src kinase and RhoGTPase activation [29].

Bovine retinal endothelial cell culture and application of mechanical strain

Capillary endothelial cells (ECs) were isolated from mammalian bovine retinas, similar to the isolation of

pericytes outlined previously [19]. Cells were expanded until passage 12–15 and seeded onto prepared TC-PDMS molds, just after corona treatment, in Dulbecco's modified Eagle's Medium (DMEM) supplemented with 10% Bovine Calf Serum (BCS; #C8056, Sigma). Prior to cell seeding, the PDMS device was clamped at either end of a customized external strain device (figure 1(A)), and extended manually with a micrometer to remove slack from the molded PDMS sheet and ensure that subsequent displacement of one end of the PDMS device would result in material strain within the PDMS molds. We refer to this as the clamped, unstrained configuration. Cells from post-confluent monolayers were trypsinized and then seeded onto these clamped, unstrained PDMS substrata. As indicated in Supporting Information (SI) Fig. S2, ECs were seeded at approximately 10^5 cells cm^{-2} to ensure formation of a confluent monolayer within <24 h, and maintained in growth medium (10% BCS in DMEM), at 5% CO_2 and 37 °C. After visual verification of a monolayer, cells were then serum starved by exchanging the growth medium with reduced serum medium, 0.5% BCS in DMEM. Serum depletion facilitated growth-arrest and cell cycle synchronization of the confluent monolayer within each well. After 24 h of serum starvation, tensile strain of the TC-PDMS substratum of each cell-seeded well was generated the by applying 10% increase in the length of the clamped TC-PDMS device. Cell response was monitored at constant (static) applied engineering strain of 10% for 15 min, 90 min, and 4 h, and cells were fixed (under strain) and stained (upon removal of strain) for subsequent analysis. These time points were selected to identify the earliest time point by which the strain cue resulted in statistically significant changes in cell cycle response, and 15 min was considered the earliest possible time point via the method of EdU incorporation. The two later time points then verified whether the system (cells and/or extracellular materials) significantly relaxed and mitigated a response to this mechanical cue on the timescale of hours. Each mold comprised 16 replicate wells per condition, as defined by strain magnitude and duration; figure 1(H) comprises data from 12 such independent experiments.

Immunocytochemistry

To determine whether strain-induced entry into S-phase of the cell cycle, an EdU assay was conducted (Click-iT® EdU Alexa Fluor 488 Imaging Kit, C10337, Molecular Probes). Briefly, cells were incubated for 90 min or 4 h at 37 °C and 5% CO_2 with 5-ethynyl-2-deoxyuridine (EdU). For strain assays of 15 min duration that included EdU, cells were pre-incubated with EdU for 1 h before replacement with full media (10% BCS) and immediate application of strain. Cells were then fixed using 4% formaldehyde (#43368 AlfaAesar Ward Hill, MA) in PBS for 15 min at room

temperature. Following fixation, cells were washed briefly with PBS (and, for anti-p27 staining, also 0.05% Tween-20 (#P1176 Teknova Hollister, CA), and permeabilized for 3 min at room temperature with 0.1% Triton X-100 (Fluka 93443, Switzerland). Cells were rinsed twice with 3% BSA and incubated for 30 min with the EdU Click-iT reaction cocktail, including the Alexa Fluor azide, as described by the manufacturer, as well as an anti-p27^{kip1} antibody (ab7961, Abcam Inc., Cambridge, MA); figure 2 shows results at 90 min post-strain. Cells were washed three times (10 min each) with PBS and imaged by fluorescence microscopy (IX-81, Olympus America, Inc.) and captured using Slidebook 5.0 (Intelligent Imaging Innovations, Inc. Denver, CO). Cell nuclei were also counterstained with 4′,6-diamidino-2-phenylindole (DAPI) (Millipore 90229, 1:2000) before imaging. The fraction of cells in DNA synthesis, or S-phase, was characterized for each condition.

Sprouting assays

ECs were seeded onto TC-PDMS substrata at post-confluent densities, as described above. After 24 h post-seeding, the EC monolayer was serum depleted for an additional 24 h by removing the 10% BCS growth media and adding DMEM with 0.5% BCS. After serum depletion for 24 h, protein solutions in reduced serum media (0.5% BCS) were added to form a gel atop the cell monolayer. Monolayer stability was promoted by addition of 100 u of 0.5% BCS in DMEM containing 3 μg ml^{-1} Collagen Type-I (Rat Tail BD Biosciences #354236) to each well and incubated at 37 °C for 30 min. The collagen solution was carefully aspirated before the addition of 150 ul of a mixture that comprised 50 vol% Growth-Factor Reduced Matrigel™ Matrix (BD Biosciences #354230), 16 vol-% Collagen Type-I (Rat Tail BD Biosciences #354236), 4 vol% FITC-conjugated Collagen Type-I (AnaSpec #85111), and 30 vol% 0.5% BCS in DMEM. After 2 h of gelation, 100 ul of 10% BCS DMEM was added to each well. Either 0% or 10% uniaxial static strain was applied to the TC-PDMS devices and over 48 h under otherwise identical incubator conditions. After 48 h, gels were carefully fixed using a 2% paraformaldyhde:1% glutaraldehyde solution for 20 min Gels were rinsed in 150 mM NaCl PBS (hereafter, PBS) before the addition of 0.1% Triton X-100 for permeabilization for 15 min Gels were again rinsed in PBS before DAPI nuclear counterstaining and Alexa Fluor 594 phalloidin (Life Technologies #A12381) in 3% bovine serum albumin in PBS. Gels were then rinsed twice in PBS before imaging. The number of sprouts and number of cells within each well was quantified using fluorescence microscopy (IX-81, Olympus America, Inc.) and captured using Slidebook 5.0 (Intelligent Imaging Innovations, Inc. Denver, CO). To visualize the sprouts in 3D, the sprouts in gels were taken to be imaged using confocal microscopy
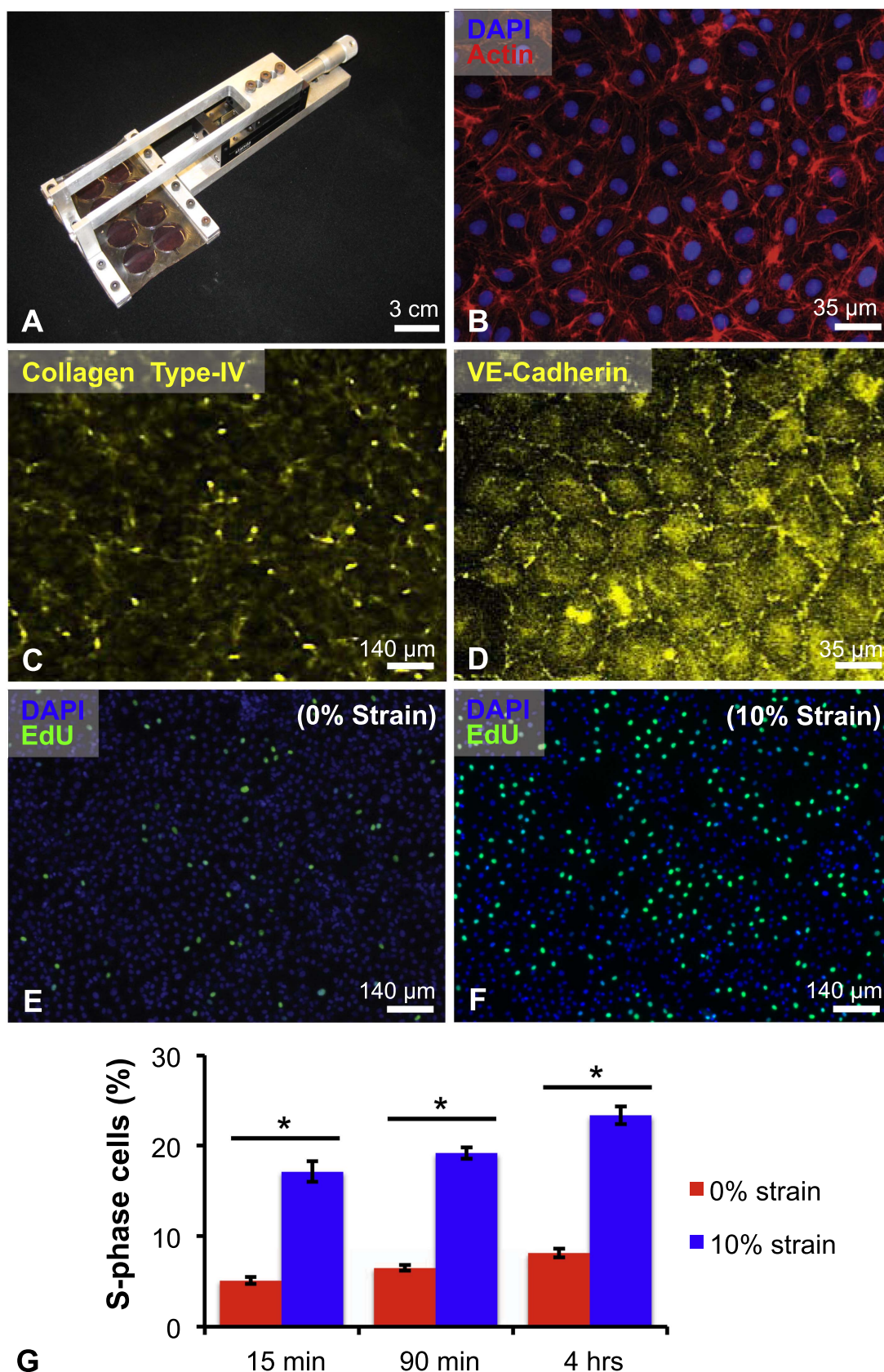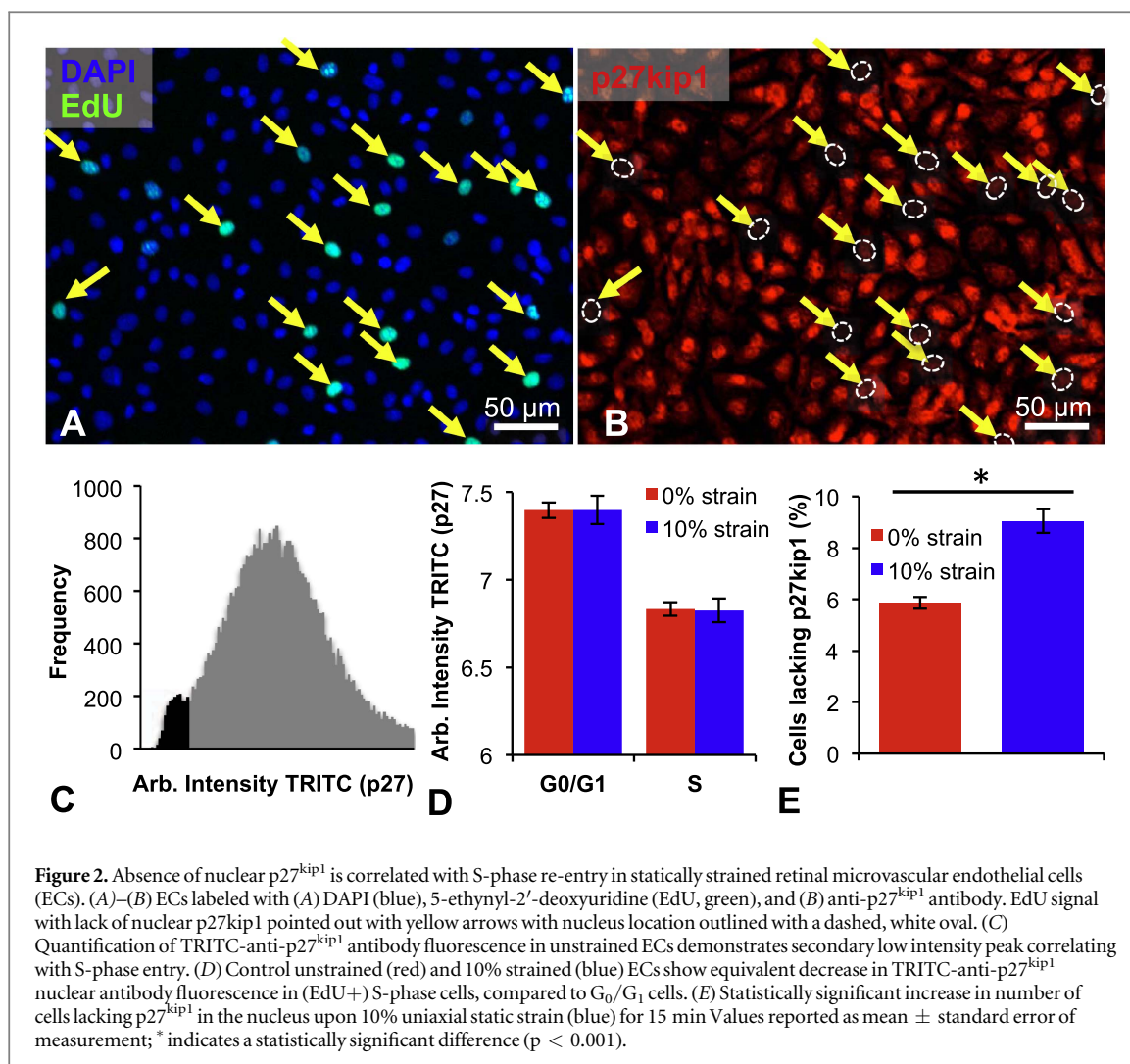
Figure 1. Static strain induces S-phase entry in quiescent retinal microvascular endothelial cells (ECs). (*A*) Multi-well elastomeric uniaxial strain device. (*B*) Bovine retinal ECs labeled nucleus via DAPI (blue) and F-actin via phalloidin (red). Antibody-stained ECs for (*C*) VE-cadherin confirmed confluence prior to strain application. (*D*) Type-IV collagen, an anticipated extracellular matrix component of ECs, visualized via antibody labeling. (*E*)–(*F*) 5-ethynyl-2′-deoxyuridine (EdU, green) incorporation and nucleus labeling via DAPI (blue) for control condition of (*E*) 0% strain and (*F*) 10% uniaxially strained EC monolayers. (*G*) Quantification of percent cells in S-phase after 15 min, 90 min, and 4 h. Values reported as mean $\pm$ standard error of measurement; * indicates statistically significant difference ($p < 0.001$).

Figure 2. Absence of nuclear p27^{kip1} is correlated with S-phase re-entry in statically strained retinal microvascular endothelial cells (ECs). (*A*)–(*B*) ECs labeled with (*A*) DAPI (blue), 5-ethynyl-2′-deoxyuridine (EdU, green), and (*B*) anti-p27^{kip1} antibody. EdU signal with lack of nuclear p27kip1 pointed out with yellow arrows with nucleus location outlined with a dashed, white oval. (*C*) Quantification of TRITC-anti-p27^{kip1} antibody fluorescence in unstrained ECs demonstrates secondary low intensity peak correlating with S-phase entry. (*D*) Control unstrained (red) and 10% strained (blue) ECs show equivalent decrease in TRITC-anti-p27^{kip1} nuclear antibody fluorescence in (EdU+) S-phase cells, compared to G$_0$/G$_1$ cells. (*E*) Statistically significant increase in number of cells lacking p27^{kip1} in the nucleus upon 10% uniaxial static strain (blue) for 15 min Values reported as mean ± standard error of measurement; * indicates a statistically significant difference ($p < 0.001$).

(Olympus FV-100, Olympus America, Inc.). The 3D stacks were then rendered using Fiji (or ImageJ, NIH).

Results and discussion

Static mechanical strain induces endothelial cell cycle re-entry

To address whether mechanical strain consistent with pericyte contraction could influence endothelial growth and anigogenic activation, we designed and fabricated a device (figure 1(A)) that applies uniform, uniaxial strain of duration and magnitude consistent with that measured previously for contractile pericytes [17]; see Methods and SI for further details. This approach—by which cells adhere to hydrophilic, optically transparent, tissue culture polydimethylsiloxane multi-well membranes (TC-PDMS)—permits live imaging during strain, immunocytochemical characterization, and isolation of mechanical cues from other potential EC stimuli. Importantly, this approach also enables application of mechanical tension to EC in the absence of pericytes (or other cell types), and thus facilitates analysis of this mechanical deformation or strain in the absence of several

competing factors possible in co-culture models (e.g., pericyte-secreted factors, EC-pericyte contact, ECM remodeling). To these ends, we seeded EC at post-confluent densities to achieve a growth-arrested population upon cell- and substratum-dependent contact ($\sim 10^5$ cells cm^{-2}). We then applied a static, sustained tensile strain comparable to pericyte-generated deformation that has been quantified directly *in vitro* [17]. At the initiation of each experiment, the growth-arrest and post-confluent nature of the microvascular EC populations were confirmed via live cell and fluorescence imaging of cortical actin, collagen-IV [30] and VE-cadherin [29] (figures 1(B)–(D)); previous studies have shown that EC growth inhibition and cell cycle arrest are induced by cell-cell contact [31]. Serum depletion 24 h post-plating promoted growth-arrest and cell cycle exit prior to the initiation of strain. Concomitant with strain induction, ECs were subjected to a media replacement and pulse-labeling with 5-ethynyl-2′-deoxyuridine (EdU); unstrained EC monolayers were prepared and manipulated identically and served as controls. As shown in figure 1, application of static strain rapidly induced a quantifiable and reproducible increase in endothelial S-phase

entry, observed as a significant elevation in nuclear EdU incorporation (figures 1(E)–(G), p < 0.001). This shift occurred within 15 min post-strain and persisted over all strain durations considered (n = 12 independent experiments, with N = 16 wells per condition in each trial). For example, by 15 min post-strain, S-phase entry increased approximately three-fold, representing ~20% of the EC population. It should be noted that these results are for growth-arrested confluent ECs, and that subconfluent ECs absent of significant cell-cell contact did not exhibit such increases in post-strain endothelial S-phase entry (data not shown).

Our finding that a modest (10%) static tensile strain can stimulate S-phase entry in microvascular ECs is consistent with recent studies demonstrating that non-physiologic, static strains of 40% could enhance 5-Bromo-2′-deoxyuridine (BrdU) incorporation in bovine pulmonary aortic ECs after 24 h; whether confluence was attained before strain application was not stated [29]. Our demonstration of EC S-phase entry within minutes following application of static uniaxial strain also aligns well with Xiong *et al*'s recent finding that human umbilical vein and arterial ECs secreted Weibel-Palade bodies (WPBs) within 15 min post-equibiaxial strains of 20–50% (equal strain in both x- and y-directions) [32]. Further, Suzuma *et al* noted that straining retinal microvascular ECs induced rapid ERK phosphorylation and mRNA expression of vascular endothelial growth-factor receptor-2 [33, 34]. To our knowledge this is the first direct demonstration that the application of static tensile strain induces endothelial S-phase re-entry in previously growth-arrested EC monolayers.

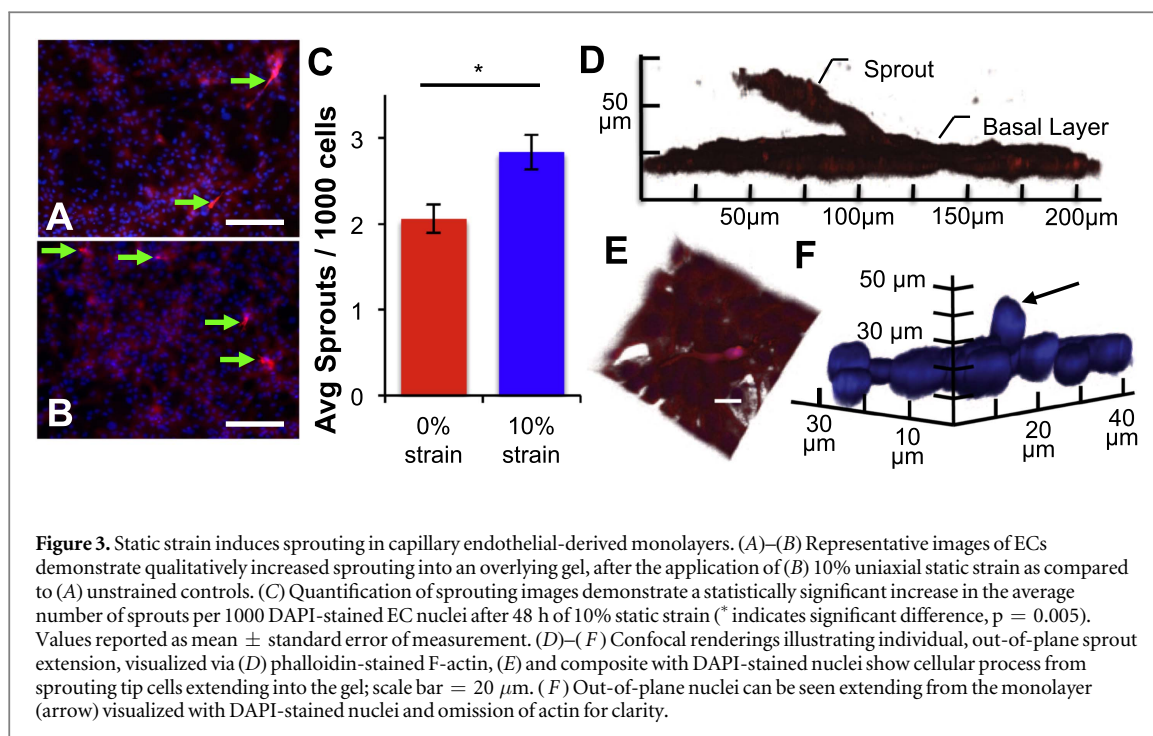### Response to mechanical strain indicated by loss of nuclear p27

It has been demonstrated that EC cell cycle progression is modulated in G_1 by several cyclin-dependent kinase inhibitors, including p16, p21 and p27. Further, recent work has revealed that cyclic strain influences EC proliferation via signaling pathways upstream of $p27^{kip1}$ [35–37]. Thus, to ascertain whether the application of modest static strain fosters endothelial cell cycle re-entry by perturbing p27 equilibrium dynamics in an S-phase dependent manner, we strained growth-arrested EC monolayers as described and monitored p27 localization via immunofluorescence. This assay revealed a distinct absence of nuclear $p27^{kip1}$ in those cells that were EdU-positive (figures 2(A)–(B)). Intensity histograms and direct imaging of fluorescently labeled $p27^{kip1}$ (figures 2(C)–(D)) highlight the correlation between S-phase re-entry (EdU-positive) and the paucity of nuclear $p27^{kip1}$ localization. These findings implicate $p27^{kip1}$ as an indicator of strain-induced S-phase entry by growth-arrested EC monolayers. Importantly, ECs subjected to 10% uniaxial strain also exhibited a statistically significant increase in the

fraction of cells lacking nuclear $p27^{kip1}$ (figure 2(E), p < 0.001). We believe that while only approximately 10% of the population lacked nuclear $p27^{kip1}$ in the presence of 10% uniaxial strain (as compared to approximately 5% in the absence of uniaxial strain), these ECs were otherwise growth-arrested, and this statistically significant increase is indicative of the potential for EC sprouting.

Mechanical strain promotes endothelial cell sprouting

Strain-stimulated cell cycle progression is necessary but insufficient to demonstrate re-proliferation or angiogenic activation. To consider whether this static strain was also sufficient to induce angiogenic activation or 'switching' in the absence of the pericytes, we applied 10% static strain to post-confluent EC monolayers within model ECM gels. In these assays, growth-factor reduced Matrigel provided a commonly used basement membrane analogue or extracellular matrix into which cells could extend from the monolayer, and this additional potential for biochemical cues was maintained constant in paired control experiments for which no strain was applied. Evidence of sprouting was quantified at 48 h for both post-strained and unstrained controls, via confocal microscopy following fixation and staining with nuclear- and cytoskeletal-specific markers. This strain resulted in 40% more sprouts from the post-confluent EC monolayer (figures 3(A)–(C)), with a statistically significant increase compared with unstrained controls (p = 0.0005). This relative enhancement of sprouting in the strained wells is notable in that any increase in sprouting from the post-confluent EC monolayer can be attributed chiefly to the applied mechanical strain. Biochemical cues may also play a synergistic role in promoting sprouting due to the required use of extracellular matrix-based gels containing low but finite growth factor, but are kept constant across strained and unstrained conditions. Figure 3(D) shows a representative image of sprouting cells from one of three replicate experiments (each with N ⩾ 10 wells per strained and unstrained condition).

The characteristic branched morphology of sprout-leading tip cells was noted consistently in strained conditions (figures 3(A)–(B), arrows), and confocal x-z analysis was conducted to confirm that ECs extended from the original growth substratum. Figures 3(D)–(E) and Supporting figure S1 show endothelial sprouts that extended many cell lengths from the original, post-confluent EC monolayer; the most distant cells along that sprout exhibited protrusions often associated with angiogenic tip cells (figures 3(D)–(E)). Nuclei were observed out-of-plane of the monolayer, suggesting that entire cells had begun to sprout upwards (figure 3(F)). Renderings of data collected in z-stacks and as movies featuring 3D-rotation confirmed these observations: continuous and connected fluorescent

Figure 3. Static strain induces sprouting in capillary endothelial-derived monolayers. (*A*)–(*B*) Representative images of ECs demonstrate qualitatively increased sprouting into an overlying gel, after the application of (*B*) 10% uniaxial static strain as compared to (*A*) unstrained controls. (*C*) Quantification of sprouting images demonstrate a statistically significant increase in the average number of sprouts per 1000 DAPI-stained EC nuclei after 48 h of 10% static strain (* indicates significant difference, p = 0.005). Values reported as mean ± standard error of measurement. (*D*)–(*F*) Confocal renderings illustrating individual, out-of-plane sprout extension, visualized via (*D*) phalloidin-stained F-actin, (*E*) and composite with DAPI-stained nuclei show cellular process from sprouting tip cells extending into the gel; scale bar = 20 μm. (*F*) Out-of-plane nuclei can be seen extending from the monolayer (arrow) visualized with DAPI-stained nuclei and omission of actin for clarity.

signals track cells from the post-confluent monolayer along the sprout lengths (Supp. Movies S1 and S2). In both z-stacks, a continuous signal was indicated in all z-planes, i.e., cells extended from the monolayer. These findings suggest that modest, static strain is sufficient to promote EC sprouting and angiogenic activation *in vitro*.

Angiogenesis is characterized fully by lumen-containing tube structures formed by the endothelial cells. Although we observed continuity of the multi-cell extensions from the strained monolayers, full confirmation of a patent lumen was not possible at such early sprouting time points. For 3D culture systems similar to our own, *in vitro* sprouting orthogonal to isolated endothelial cell monolayers typically requires longer time scales with patent lumen formation only observed after many days in culture [38–40]. However, we have previously demonstrated lumen formation in the same cell type [40], suggesting that our sprout-like structures may form observable lumens at longer time scales. In contrast, rapid formation of capillary-like structures with lumen-containing regions has been demonstrated previously to occur within 2 days for purified ECs on top of (rather than within) Matrigel [41], or for more complex tissue explants [38, 42]. Most studies that observe lumen-containing capillary structures use bioactive or exogenous factors in order to induce, expedite, and stabilize angiogenic sprouting [38–42]. In order to decouple mechanical from chemical cues, we minimized exogenous factors other than those contained in the Matrigel, and focused on independent effects of strain on early sprout formation.

Summary and outlook

Initial vessel destabilization is generally attributed to a disrupted balance among several biochemical cues, including those derived from vascular and non-vascular cells. These include but are not limited to growth and survival factor (and cognate receptor) expression/release, protease activation/expression or cell-matrix receptor dynamics [43, 44], which may coordinate angiogenic activation and microvascular morphogenesis. Indeed, we observe EC cell cycle re-entry and response to static strains consistent with that generated by capillary pericytes [17]. Our study is in agreement with previous *ex vivo* studies of whole vessels (arterial trunks and carotid arteries) demonstrating that excised capillaries and microvessels could be driven into proliferative states via uniaxial extension [45]. In other microvascular or macrovessel contexts, strain could be generated by other nearby non-vascular or vascular cell types such as fibroblasts or vascular smooth muscle cells [11–13], and others have shown that induced injuries *in vivo* can result in both interstitial fibroblasts contraction of gels and modulation of neovascularization [12, 13]. However, in the context of microvascular remodeling and angiogenic activation considered here, pericytes do play a predominant role. The perivascular location of contractile pericytes that encircle the capillary presents the potential for cell-generated force to exert an effective tensile (hoop) strain on those ECs that are in close proximity or direct contact within the basement membrane [17]. Separately, unstrained co-cultures of ECs and pericytes within collagen gel punch-wound assays have demonstrated that increased pericyte

contractility (via molecular manipulation of the myosin phosphatase RhoGTPase interacting protein) correlated with increased EC sprouting [26]. Durham *et al* also showed that an increased number of heterotypic gap junctions between ECs and pericytes in co-culture does not by itself promote angiogenic sprouting [46]. This suggests that pro-angiogenic EC responses can be mediated by cell contact-dependent and soluble mechanisms, as well as by strain generated by adjacent cells such as contractile pericytes. Of course, it remains an important topic of future study whether and to what extent pericyte-generated strain may modulate angiogenic switching via cell-cell contact, non-vascular or vascular cell-cell type crosstalk, or release of angiogenic effectors from contractile pericytes and/or strained ECs. The present data suggest that pericyte contractility, reversal of endothelial growth arrest, and angiogenic activation are chemomechanically coupled.

Our results are distinct from and complement previous *in vitro* and *in vivo* studies, which have focused either on non-confluent (i.e., proliferating and migrating) ECs or in more complex *in vivo* settings. For example, static strain has been shown to alter extracellular matrix (ECM) organization and, thus, direct cell migration through contact guidance-dependent mechanisms [9–11], although it has been debated whether cells align in parallel [9, 11] or are perpendicular [10] to the applied strain. Krishnan *et al* inserted microvessel fragments (with ECs and perivascular cells) within gels and then applied strain *in vitro*; they found that neither applied static or cyclic strain of a lower magnitude (6%) than considered herein (10%) promoted a statistically significant increase in the number of vessels compared to unstrained constructs end-clamped in the same manner [8]. Boerkel *et al* and Kilarski *et al* reported *in vivo* experiments of wound models that disrupted existing vasculature; neither study actively strained pre-encapsulated cells within the implanted gels. Boerkel *et al* showed instead that propensity for vascular invasion into a gel depends on whether and how long a mechanical constraint (boundary condition) is imposed on the gels. Kilarski *et al* showed that increased gel deformability (stiffness via varied gel composition) correlated with increased vascular invasion; the authors hypothesized that cell-mediated contraction (by fibroblasts) was necessary for vascular ingrowth and network remodeling, noting that they did not observe new sprouting. Such *in vivo* studies are interesting and interchangeably discuss 'constraints' and 'tension' as mediators of vascular remodeling, but were not designed to decouple mechanical cues from biochemical signals; the mechanical cues are not well-defined or controlled. Further, these previous studies have demonstrated increased cell alignment and in some cases, increased proliferation in response to constraints or strain, but none has shown the impact that straining a quiescent, post-confluent microvascular endothelial cell population can have on increasing or modulating angiogenic activation and sprouting dynamics. The simple strain state applied herein to confluent monolayers reflects the physiological stretch in microvessels. It is not intended to reflect further complexities such as distention or the fluid shear and cyclic deformation anticipated for larger vessels. This approach enables straightforward consideration of a key strain state anticipated in microvessels encircled by contractile cells such as pericytes.

We demonstrate that when mechanical strain applied to endothelial cells that are in a post-confluent and growth-arrested monolayer, ECs are activated and re-enter the cell cycle. This strain also promotes angiogenic activation and capillary-like endothelial sprouting. These findings that the isolated factor of static strain on post-confluent EC monolayers can induce such phenotypic changes also informs our understanding of pathological angiogenesis, such as that during diabetic retinopathy [47, 48]. Pericyte loss is considered a hallmark of this condition, and pericyte dropout has been correlated with the onset of undesirable angiogenesis within the eye. However, our results suggest that pericyte contraction and attendant strain of the EC environment—rather than pericyte death or loss, and separately from any other pericyte signaling roles—can serve as an early mechanical cue that fosters re-activation of the endothelial cell cycle progression. Strain can be communicated to ECs via cell-generated contraction by pericytes in microvessels, and also by other contractile perivascular cell types such as vascular smooth muscle cells in more mature vessels. This mechanical form of an 'angiogenic switch', due to contraction of nearby cells including but not limited to pericytes and independently of pulsatile fluid shear flow, prompts renewed consideration of how even modest and static mechanical strain can rapidly modulate EC growth dynamics and angiogenic status.

Acknowledgments

References

[1] Berceli S A, Borovetz S and Sheppeck R A 1991 Mechanisms of vein graft atherosclerosis: LDL metabolism and endothelial actin reorganization *J. Vasc. Surg.* **13** 336–47

[2] Wong A J, Pollard T D and Herman I M 1983 Actin filament stress fibers in vascular endothelial cells *in vivo Science* **219** 867–9

[3] Ando J and Yamamoto K 2011 Effects of shear stress and stretch on endothelial function *Antioxid. Redox Signal.* **15** 1389–403

[4] Sumpio B E, Chang R, Xu W J, Wang X J and Du W 1997 Regulation of tPA in endothelial cells exposed to cyclic strain: role of CRE, AP-2, and SSRE binding sites *Am. J. Physiol.* **273** C1441–8

[5] Shukla A, Dunn A R, Moses M A and Van Vliet K J 2004 Endothelial cells as mechanical transducers: enzymatic activity and network formation under cyclic strain *Mech. Chem. Biosyst.* **1** 279–90

[6] Ikeda M, Takei T, Mills I, Kito H and Sumpio B E 1999 Extracellular signal-related kinases 1 and 2 activation in endothelial cells exposed to cyclic strain *Am. J. Physiol.* **276** H614–22

[7] Yung Y C, Chae J, Buehler M J, Hunter C P and Mooney D J 2009 Cyclic tensile strain triggers a sequence of autocrine and paracrine signaling to regulate angiogenic sprouting in human vascular cells *Proc. Natl. Acad. Sci. USA* **106** 15279–84

[8] Krishnan L, Underwood C J, Maas S, Ellis B J, Kode T C, Hoying J B and Weiss J A 2008 Effect of mechanical boundary conditions on orientation of angiogenic microvessels *Cardiovasc. Res.* **78** 324–32

[9] Matsumoto T, Sasaki J-I, Alsberg E, Egusa H, Yatani H and Sohmura T 2007 Three-dimensional cell and tissue patterning in a strained fibrin gel system *PLoS One* **2** e1211

[10] Matsumoto T, Yung Y C, Fischbach C, Kong H J, Nakaoka R and Mooney D J 2007 Mechanical strain regulates endothelial cell patterning *in vitro Tissue Eng.* **13** 207–17

[11] Korff T and Augustin H G 1999 Tensional forces in fibrillar extracellular matrices control directional capillary sprouting *J. Cell Sci.* **3258** 3249–58

[12] Boerckel J D, Uhrig B A, Willett N J, Huebsch N and Guldberg R E 2011 Mechanical regulation of vascular growth and tissue regeneration *in vivo Proc. Natl Acad. Sci. USA* **108** E674–80

[13] Kilarski W W, Samolov B, Petersson L and Kvanta A 2009 Biomechanical regulation of blood vessel growth during tissue vascularization **15** 657–65

[14] Kutcher M E and Herman I M 2009 The pericyte: cellular regulator of microvascular blood flow *Microvasc. Res.* **77** 235–46

[15] Udan R S, Culver J C and Dickinson M E 2013 Understanding vascular development *Wiley Interdiscip. Rev. Dev. Biol.* **2** 327–46

[16] Armulik A, Genove G and Betsholtz C 2011 Pericytes: developmental, physiological, and pathological perspectives, problems, and promises *Dev. Cell* **21** 193–215

[17] Lee S, Zeiger A, Maloney J M, Kotecki M, Van Vliet K J and Herman I M 2010 Pericyte actomyosin-mediated contraction at the cell-material interface can modulate the microvascular niche *J. Phys. Condens. Matter* **22** 194115

[18] Kotecki M, Zeiger A S, Van Vliet K J and Herman I M 2010 Calpain- and talin-dependent control of microvascular pericyte contractility and cellular stiffness *Microvasc. Res.* **80** 339–48

[19] Herman I M and D'Amore P A 1985 Microvascular pericytes contain muscle and nonmuscle actins *J. Cell Biol.* **101** 43–52

[20] Kutcher M E, Kolyada A Y, Surks H K and Herman I M 2007 Pericyte Rho GTPase mediates both pericyte contractile phenotype and capillary endothelial growth state *Am. J. Pathol.* **171** 693–701

[21] De Oliveira F 1966 Pericytes in Diabetic Retinopathy *Br. J. Ophthalmol.* **50** 134–44

[22] Orlidge A and D'Amore P A 1987 Inhibition of capillary endothelial cell growth by pericytes and smooth muscle cells *J. Cell Biol.* **105** 1455–62

[23] Cogan D G, Toussaint D and Toichiro K 1961 Retinal vascular patterns: iv. Diabetic retinopathy *Arch. Ophthalmol.* **66** 366–78

[24] Cai J and Boulton M 2002 The pathogenesis of diabetic retinopathy: old concepts and new questions *Eye* **16** 242–60

[25] Baluk P, Hashizume H and M D M 2005 Cellular abnormalities of blood vessels as targets in cancer *Curr. Opin. Genet. Dev.* **15** 102–11

[26] Durham J T, Surks H K, Dulmovits B M and Herman I M 2014 Pericyte contractility controls endothelial cell cycle progression and sprouting: insights into angiogenic switch mechanics *AJP Cell Physiol.* **307** C878–92

[27] Vickers J A, Caulum M M and Henry C S 2006 Generation of hydrophilic poly(dimethylsiloxane) for high-performance microchip electrophoresis *Anal. Chem.* **78** 7446–52

[28] Feinberg A W, Schumacher J F and Brennan A B 2009 Engineering high-density endothelial cell monolayers on soft substrates *Acta Biomater.* **5** 2013–24

[29] Liu W F, Nelson C M, Tan J L and Chen C S 2007 Cadherins, RhoA, and Rac1 are differentially required for stretch-mediated proliferation in endothelial versus smooth muscle cells *Circ. Res.* **101**

[30] Davis G E and Senger D R 2005 Endothelial extracellular matrix: biosynthesis, remodeling, and functions during vascular morphogenesis and neovessel stabilization *Circ. Res.* **97** 1093–107

[31] Vinals F and Pouyssegur J 1999 Confluence of vascular endothelial cells induces cell cycle exit by inhibiting p42/p44 mitogen-activated protein kinase activity *Mol Cell. Biol.* **19** 2763–72

[32] Xiong Y *et al* 2013 Hypertensive stretch regulates endothelial exocytosis of Weibel-Palade bodies through VEGF receptor 2 signaling pathways *Cell Res.* **23** 1–15

[33] Suzuma I, Hata Y, Clermont A, Pokras F, Rook S L, Suzuma K, Feener E P and Aiello L P 2001 Cyclic stretch and hypertension induce retinal expression of vascular endothelial growth factor and vascular endothelial growth factor receptor-2: potential mechanisms for exacerbation of diabetic retinopathy by hypertension *Diabetes* **50** 444–54

[34] Suzuma I, Suzuma K, Ueki K, Hata Y, Feener E P, King G L and Aiello L P 2002 Stretch-induced retinal vascular endothelial growth factor expression is mediated by phosphatidylinositol 3-kinase and protein kinase C (PKC)-?? but not by stretch-induced ERK1/2, Akt, Ras, or classical/novel PKC pathways *J. Biol. Chem.* **277** 1047–57

[35] Besson A, Gurian-West M, Schmidt A, Hall A and Roberts J M 2004 p27Kip1 modulates cell migration through the regulation of RhoA activation *Genes Dev.* **18** 862–76

[36] Huang S, Chen C S and Ingber D E 1998 Control of cyclin D1, p27(Kip1), and cell cycle progression in human capillary endothelial cells by cell shape and cytoskeletal tension *Mol. Biol. Cell* **9** 3179–93

[37] Mammoto A, Huang S, Moore K, Oh P and Ingber D E 2004 Role of RhoA, mDia, and ROCK in cell shape-dependent control of the Skp2-p27kip-1 pathway and the G1/S transition *J. Biol. Chem.* **279** 26323–30

[38] Kleinman H K and Martin G R 2005 Matrigel: basement membrane matrix with biological activity *Semin. Cancer Biol.* **15** 378–86

[39] Nakatsu M N, Sainson R C A, Aoto J N, Taylor K L, Aitkenhead M, Pérez-del-Pulgar S, Carpenter P M and Hughes C C W 2003 Angiogenic sprouting and capillary lumen formation modeled by human umbilical vein endothelial cells (HUVEC) in fibrin gels: the role of fibroblasts and Angiopoietin-1★ *Microvasc. Res.* **66** 102–12

[40] Demidova-Rice T N, Geevarghese A and Herman I M 2011 Bioactive peptides derived from vascular endothelial cell extracellular matrices promote microvascular morphogenesis and wound healing in vitro *Wound Repair Regen.* **19** 59–19

[41] Kubota Y, Kleinman H K, Martin G R and Lawley T J 1988 Role of laminin and basement membrane in the morphological differentiation of human endothelial cells into capillary-like structures *J. Cell Biol.* **107** 1589–98

[42] Auerbach R, Lewis R, Shinners B, Kubai L and Akhtar N 2003 Angiogenesis assays: a critical overview *Clin. Chem.* **49** 32–40

[43] Norrby K 1997 Angiogenesis: new aspects relating to its initiation and control *APMIS* **105** 417–37

[44] Rundhaug J E 2005 Matrix metalloproteinases and angiogenesis angiogenesis review series *J. Cell. Mol. Med.* **9** 267–85

[45] Lee Y-U, Drury-Stewart D, Vito R P and Han H-C 2008 Morphologic adaptation of arterial endothelial cells to longitudinal stretch in organ culture *J. Biomech.* **41** 3274–7

[46] Durham J T, Dulmovits B M, Cronk S M, Sheets A R and Herman I M 2015 Pericyte chemomechanics and the angiogenic switch: insights into the pathogenesis of proliferative diabetic retinopathy? *Investig. Ophthalmol. Vis. Sci.* **56** 3441–59

[47] Hammes H P, Lin J, Renner O, Shani M, Lundqvist A, Betsholtz C, Brownlee M and Deutsch U 2002 Pericytes and the pathogenesis of diabetic retinopathy *Diabetes* **51** 3107–12

[48] Hammes H-P 2005 Pericytes and the pathogenesis of diabetic retinopathy *Horm. Metab. Res.* **37** 39–43